Accepted Manuscript

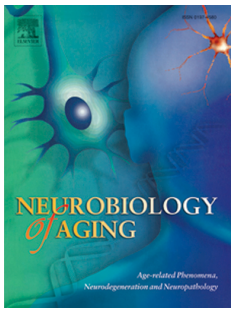

Multimodal MRI quantification of the common neurostructural bases within the FTD-ALS continuum

Chiara Crespi, Alessandra Dodich, Stefano F. Cappa, Nicola Canessa, Sandro Iannaccone, Massimo Corbo, Christian Lunetta, Andrea Falini, Chiara Cerami

PII: S0197-4580(17)30315-9

DOI: 10.1016/j.neurobiolaging.2017.09.019

Reference: NBA 10039

To appear in: *Neurobiology of Aging*

Received Date: 17 May 2017

Revised Date: 15 September 2017

Accepted Date: 19 September 2017

Please cite this article as: Crespi, C., Dodich, A., Cappa, S.F., Canessa, N., Iannaccone, S., Corbo, M., Lunetta, C., Falini, A., Cerami, C., Multimodal MRI quantification of the common neurostructural bases within the FTD-ALS continuum, *Neurobiology of Aging* (2017), doi: 10.1016/j.neurobiolaging.2017.09.019.

Multimodal MRI quantification of the common neurostructural bases within the FTD-ALS continuum

Chiara Crespi [1]*, Alessandra Dodich[2,3], Stefano F. Cappa[4,5], Nicola Canessa[2,4], Sandro Iannaccone[2,3], Massimo Corbo[6], Christian Lunetta[7], Andrea Falini[2,8,9], and Chiara Cerami[2,3,9].

Affiliations

[1] Institute of Biomedical Technologies, National Research Council, Segrate, Italy

[2] Division of Neuroscience, San Raffaele Scientific Institute, Milano, Italy

[3] Department of Clinical Neurosciences, IRCCS San Raffaele Turro, Milano, Italy

[4] NeTS Center, Scuola Universitaria Superiore IUSS Pavia, Pavia, Italy

[5] IRCCS Fatebenefratelli di Brescia, Brescia, Italy

[6] Department of Neurorehabilitation Sciences, Casa Cura Policlinico, Milano, Italy

[7] NEuroMuscolar Omnicentre, Fondazione Serena Onlus, Niguarda Ca' Granda Hospital, Milano, Italy

[8] Neuroradiology Unit, San Raffaele Scientific Institute, Milano, Italy

[9] Vita-Salute San Raffaele University, Milano, Italy

*Corresponding author: Chiara Crespi

Institute of Biomedical Technologies, National Research Council (CNR)

E-mail: chiara.crespi@itb.cnr.it

Street address: Via Fratelli Cervi 93, 20090, Segrate (MI), Italy

Phone: +39.02.26422629

Abstract

The continuum hypothesis linking the behavioral variant of Frontotemporal Dementia (bvFTD) and Amyotrophic Lateral Sclerosis (ALS) is supported by clinical, pathological, genetic and neuroimaging evidence. In the present multimodal magnetic resonance study, we characterized the site and extent of shared neurostructural changes in gray and white matter in 20 bvFTD and 19 ALS patients without dementia.

We found an overlap of macrostructural and microstructural damage in both patient groups compared to healthy controls, involving the right orbital and the bilateral anterior cingulate cortices, the corticospinal tract and corpus callosum. The quantification of grey and white matter damage within the areas of shared alterations highlighted a higher degree of atrophy in orbitofrontal and frontomedial regions in patients with more severe executive and/or behavioral symptoms, and a higher degree of degeneration in the motor pathway in patients with more severe motor neuron disorders.

Our finding provides additional evidence confirming the FTD-ALS continuum hypothesis, and supports the notion of a bimodal but convergent pattern of neurostructural changes characterizing bvFTD and ALS.

Keywords

1. Behavioral variant of Frontotemporal Dementia
2. Amyotrophic Lateral Sclerosis
3. ALS-FTD Continuum Hypothesis
4. Tract-Based Spatial Statistics
5. Voxel-Based Morphometry
6. Corticospinal tract

1. Introduction

The Frontotemporal Dementia (FTD) – Amyotrophic Lateral Sclerosis (ALS) continuum hypothesis, considering FTD and ALS as extreme points of a disease spectrum, is now supported by a robust genetic and neuropathological evidence (Ferrari et al., 2011; Ling et al., 2013). Above all, the TAR DNA binding protein (TPD-43) inclusions within the central nervous system first, and then mutations in the hexanucleotide (GGGGCC) repeat expansion of the chromosome 9 open reading frame 72 (C9orf72) gene have been consistently identified in both diseases and, thus, proposed as the common neuropathological and genetic hallmarks, respectively (Lattante et al., 2015; Ling et al., 2013; Weishaupt et al., 2016).

While the clinical presentation of these neurodegenerative diseases is extremely different, a partial symptom overlap is not uncommon (Devenney et al., 2015; Lillo and Hodges, 2009). Indeed, despite the different onset sites of neurodegenerative changes in ALS and bvFTD – i.e., premotor and primary motor cortices in ALS (Turner and Verstraete, 2015), fronto-limbic and temporal regions in bvFTD (Seeley et al., 2008) – both an early extra-motor involvement in ALS (Goldstein and Abrahams, 2013), and the presence of damage of corticospinal pathway in bvFTD (Lillo et al., 2012), have been consistently documented. These findings can explain the overlap of signs and symptoms observed in clinical practice (e.g., Cerami et al., 2015b; Consonni et al., 2013), as well as the co-occurrence of the two diseases (i.e., ALS-FTD). It has been estimated that the 10-15% of patients diagnosed as FTD – and in particular those individuals receiving a diagnosis of behavioral variant of FTD (bvFTD) – can develop a motor neuron impairment, and are then diagnosed with ALS (Burrell et al., 2011; Lomen-Hoerth, 2011). Conversely, about 13-15% of ALS patients may display behavioral and/or cognitive changes typically observed in FTD, and particularly in bvFTD, satisfying the clinical criteria for FTD diagnosis (Consonni et al., 2013; Lomen-Hoerth, 2011; Phukan et al., 2012; Ringholz et al., 2005).

The continuum hypothesis is further supported by cases in which the presence of subtle motor dysfunctions in FTD, as well as non-motor alterations in ALS, do not reach the clinical significance required to make the diagnosis of ALS-FTD. For example,

neurophysiological investigations highlight about 25-30% of FTD patients present mild clinical and EMG signs not fulfilling the clinical criteria for the diagnosis of ALS (Burrell et al., 2011; Cerami et al., 2015a; Lomen-Hoerth et al., 2002). Conversely, it is recognized that some ALS patients may show behavioral alterations or cognitive impairments (i.e., ALSbi and ALSci) not fulfilling the criteria for dementia (Strong et al., 2009). Considerable advances in the understanding of the neuropsychological profile of ALS patients triggered the need for consensus criteria revision of the diagnosis of frontotemporal dysfunction in ALS (Strong et al., 2017), then resulting in the concept of the frontotemporal spectrum disorder of ALS (ALS-FTSD).

Finally, neuroimaging investigations provide further crucial evidence of the involvement of frontal and temporo-limbic regions in ALS (Abrahams et al., 2005; Lillo et al., 2012; Tsermentseli et al., 2012), suggesting a neurostructural overlap with bvFTD. This pattern involves anterior cingulate, supramarginal gyrus, premotor and motor cortices, alongside the alteration of the anterior portion of corpus callosum, the corticospinal tract and the inferior longitudinal fasciculus (Lillo et al., 2012).

A precise quantification of the conjunction pattern between bvFTD and ALS, as well as a detailed characterization of white-matter microstructural properties of commonly degenerated pathways, have not been provided yet. The aim of the present study is to measure both commonalities and differences across bvFTD and ALS compared to healthy controls (HC). This was done by means of a conjunction analysis, considering grey matter (GM) density values and white matter (WM) microstructural indices, i.e. fractional anisotropy (FA), mode of anisotropy (MO), and mean diffusivity (MD).

2. Materials and methods

2.1 Participants

Twenty patients meeting the criteria for probable bvFTD (Rascovsky et al., 2011) were enrolled in a multimodal Magnetic Resonance Imaging (MRI) study (see Table 1 for demographics and clinical information). In-depth neuropsychological, behavioral and

instrumental assessment (i.e., needle electromyography (EMG), conventional MRI and [^{18}F]FDG-PET imaging) supported the clinical classification.

The neuropsychological exam included the evaluation of language abilities (picture naming and single word comprehension), short-term (digit span forward) and long-term memory (Rey auditory verbal learning; Rey-Osterrieth complex figure recall), visuo-spatial abilities (Rey-Osterrieth complex figure copy), social cognition (Ekman 60-faces test, story-based empathy task) and executive functions (Raven colored progressive matrices; digit span backward; letter (P-F-L) and category (animals-fruits-cars) fluency; cognitive estimation task; Stroop interference test and either Wisconsin card sorting test or Weigl's sorting test). The presence of behavioral alterations was assessed with the Frontal Behavioral Inventory and the Neuropsychiatric Inventory questionnaires.

A detailed neurological examination recorded possible signs of upper (UMN) and lower (LMN) motor neuron dysfunctions (MNDs). Needle EMG evaluated neurophysiological evidence of acute and chronic neurogenic changes. Patients were thus classified as pure bvFTD or bvFTD-MNDs according to the absence/presence of MNDs, either on clinical or electromyographic evidence, as described in Cerami et al. (2015a). All bvFTD patients were tested for the presence of *C9ORF72* or *GRN* gene mutations. None of them showed pathological mutations. Exclusion criteria for bvFTD were: left-handedness, a positive medical history for other neuropsychiatric disorders, the presence of other pathological findings on MRI scans, a Mini-Mental State Examination (MMSE) raw score<21/30 and a Clinical Dementia Rating (CDR) scale global score>1.

Nineteen individuals without dementia (CDR range=0-0.5) with either probable or definite ALS diagnosis (Brooks et al., 2000) were also enrolled (Table 1). Three out of 19 patients presented bulbar onset (i.e., dysarthria and/or dysphagia), while the rest had a spinal onset. Clinical disability was assessed with the revised version of the ALS-Functional Rating Scale (ALSFRS-r) (Cedarbaum et al., 1999). All ALS patients completed a neuropsychological and behavioral assessment to evaluate the presence of cognitive and/or behavioral impairments. The testing battery was the same used for bvFTD patients (see

above) except for the Rey-Osterrieth complex figure, which was not administered to ALS patients. In order to control for individual differences in motor speed, we considered both the mean fluency indexes and the reading time-difference condition of the Stroop test. Patients with arm weakness were assisted by the examiner to move the cards during the task. Patients were thus classified as pure ALS or ALS with frontotemporal spectrum disorders (i.e., ALS-FTSD) according to Strong's criteria (Strong et al., 2017).

ALS patients were tested for the presence of *C9ORF72* or *GRN* gene mutations also, showing no pathological mutation. Exclusion criteria for ALS were: left-handedness, a positive medical history for other neuropsychiatric disorders as well as the presence of other pathological findings on MRI scans, mild respiratory disorders (forced vital capacity <70% of predicted capacity), severe dysarthria, and communication difficulties potentially invalidating the interpretation of neuropsychological performance.

Twenty healthy controls (HC) matched with patients with respect to age and gender, also participated in the study (Table 1). They were recruited from local senior community centers on a voluntary basis. None of them was taking any medication potentially interfering with neurobehavioral functioning. A next of kin (e.g., spouse) of each control subject was interviewed to corroborate his/her normal daily functioning. Exclusion criteria for HC were the presence of neuropsychiatric disorders, a positive neurologic examination, a global Clinical Dementia Rating score>0, a Mini-Mental State Examination score ≤28/30, a verbal and visuo-spatial delayed memory performance (Rey Auditory Verbal Learning test and Rey Figure Recall task) ≤25th percentile.

All participants, or relative informants, gave their written informed consent to the experimental procedure, which was approved by the Ethics Committee of the San Raffaele Hospital.

Table 1. Demographic features and disease parameters of the enrolled sample

	bvFTD (n=20)	ALS (n=19)	HC (n=20)	Stats
Age [years; mean ± sd]	66.14 ± 6.81	60.97 ± 11	60.83 ± 8.03	F(2,56)=2.61, p=0.08
Gender [m : f]	12 : 8	14 : 5	13 : 7	χ^2=0.83, p=0.66
Education [years; mean ± sd]	9.69 ± 4.53	10.3 ± 4.63	12.95 ± 4.17	F(2,56)=3.26, p=0.046
Disease duration [months; median (interquartile range)]	57 (24-84)	18 (7.5-29.75)	-	t(37)=2.3, p=0.03
ALS-FSR-r global score [mean ± sd]	46.5 ± 2.5	38.17 ± 7.54	-	t(37)=4.68, p<0.0001
CDR global score [range]	0-1	0-0.5	-	t(37)=7.3, p<0.0001

2.2 MRI data acquisition

All participants underwent a multimodal MRI scanning session, including T1-weighted and Diffusion Tensor Imaging (DTI) sequences. Fluid-Attenuated-Inversion Recovery (FLAIR) and T2-weighted images were also collected for diagnostic purposes. All MRI scans were performed using a 3T Philips Achieva scanner (Philips Medical Systems, Best, NL) with an 8-channels head coil. T1-weighted images were collected with a gradient-echo sequence (220 slices, TR = 600 ms, TE = 20 ms, in-plane resolution 0.9 x 0.9 x 0.8 mm3). Whole-brain DTI images were acquired using a single-shot echo planar sequence (TR/TE=8986/80 msec; FOV=240 mm^2; 56 sections; 2.5 mm isotropic resolution) with parallel imaging (SENSE factor=2.5) and diffusion gradients applied along 32 non-collinear directions (b-value=1000 sec/mm^2). One non-diffusion weighted volume was also collected.

2.3 VBM data preprocessing and analysis

T1-weighted structural brain images were pre-processed and quantitatively analyzed in SPM8 (http://www.fil.ion.ucl.ac.uk/spm/software/spm8/) on Matlab v7.4 (Mathworks-Inc.,

Sherborn, MA), using the VBM8 (http://dbm.neuro.uni-jena.de/vbm/download/) and Diffeomorphic Anatomical Registration Through Exponentiated Lie algebra (DARTEL) (Ashburner, 2009, 2007) toolboxes. After a bias-correction for field-intensity inhomogeneities, the T1-weighted images were registered using linear (12-parameter affine) and non-linear (warping) transformations, and tissue-classified in GM, WM and cerebrospinal fluid (CSF) components. The segmented tissue maps were then registered to the stereotactic space of the Montreal Neurological Institute (MNI) using the iterative high-dimensional normalization approach provided by DARTEL toolbox. Finally, the non-linear DARTEL normalized gray matter images were smoothed with a 8-mm Full-Width-Half-Maximum (FWHM) Gaussian-kernel and entered in the subsequent voxel-based statistical analyses.

Whole-brain analyses based on two-sample t-tests highlighted GM density differences between healthy controls and ALS and bvFTD patients separately. Then, to explore the overlap between the atrophic processes in ALS and bvFTD, we computed a conjunction analysis between the statistical maps representing the common reduction of GM in the two patient groups compared to healthy controls (Nichols et al., 2005). Total intracranial volume was used as nuisance variables in order to correct for variation in individual brain sizes. We excluded all voxels with a GM-value<0.15 (maximum=1) to avoid edge effects at the border between GM and WM. The statistical thresholds were set at $p<0.05$ Family-Wise-Error (FWE) corrected for multiple comparisons at the cluster-level. Those cerebral regions for which maps are provided were localized with reference to cytoarchitectonical probabilistic maps of the human brain, using the SPM-Anatomy toolbox v1.8 (Eickhoff et al., 2005).

2.4 DTI data preprocessing and analysis

We performed DTI data pre-processing and analysis with the FMRIB Software Library tools (FSL: http://fsl.fmrib.ox.ac.uk/fsl/fslwiki/). Single-subject datasets were first corrected for eddy current distortions and motion artifacts, skull-stripped and finally, as a result of the fitting of the diffusion tensor model at each voxel, maps of diffusion scalar

indices were generated. We then carried out DTI group analyses with Tract-Based Spatial Statistics (TBSS) (Smith et al., 2006). Briefly, the TBSS method includes a voxelwise non-linear registration of all subjects' Fractional Anisotropy (FA) maps that, once aligned, are affine-transformed on a standard space (1x1x1 mm^3 MNI152). After co-registration, FA maps are averaged to create a mean FA image, and then used to generate a mean FA tract skeleton, representing all common tracts across subjects. In order to exclude from further analysis those parts of the skeleton that could not ensure a good correspondence across subjects, we applied a threshold of 0.20 to the mean FA skeleton image. Finally, to account for residual misalignments after the initial nonlinear registration, all subjects' FA data were projected onto the thresholded mean FA skeleton, creating a 4D dataset of all subjects' FA skeletonized data, which was fed into whole-brain voxel-wise statistical analysis. In addition, we ran the non-FA TBSS script on maps of mean diffusivity (MD) and mode of anisotropy (MO).

Whole-brain voxelwise statistics were performed with *randomise*, software implemented in FSL performing a permutation-based nonparametric approach within the framework of the GLM. We employed the Threshold-Free Cluster Enhancement option (Smith and Nichols, 2009) and set the significance threshold for group differences at $p<0.05$ corrected for multiple comparisons. We tested the presence of WM microstructural changes in the two patient groups compared to controls separately – i.e., ALS *versus* HC and bvFTD *versus* HC – setting a number of 10,000 random permutations per contrast. We then used the *easythresh_conj* script to calculate the conjunction pattern between white-matter alterations highlighted in ALS and bvFTD patients. The anatomical localization of significant clusters was performed using the JHU White-Matter Tractography Atlas (Hua et al., 2008). Finally, for graphical purposes, result maps were smoothed applying a Gaussian Kernel of 3 mm via the *tbss_fill* script.

2.5 Statistical comparisons and quantification of neurostructural damage

In order to explore voxelwise results from conjunction analyses, we used an analysis of variance (ANOVA) to compare mean GM density and WM microstructural indices extracted from conjunction patterns between the two patient groups and HC.

Additionally, we used Chi-square tests to separately assess the association between GM atrophy and WM microstructural changes within the bvFTD-ALS conjunction pattern and, respectively, the presence of cognitive/behavioral symptoms in ALS patients (i.e, ALS-FTSD) and of motor symptoms in bvFTD patients (i.e., bvFTD-MNDs). Preliminarily, we classified all patients as impaired/non impaired based on the distribution of GM density and diffusion indices (i.e., FA and MO) in HC (i.e., patients whose values fell below the 5^{th} percentile of HC were considered as impaired).

Finally, in order to evaluate the percent variation of GM density and FA/MO mean indices we performed exploratory comparisons among bvFTD (i.e., pure bvFTD and bvFTD-MNDs) and ALS (i.e., pure ALS and ALS-FTSD) subgroups with HC.

Statistical analyses were carried out with Statistica software (http://www.statsoft.com).

3. RESULTS

3.1 BvFTD-ALS clinical continuum

Six out of 20 bvFTD patients showed clinical and/or EMG evidence of MNDs (i.e., bvFTD-MNDs), not satisfying criteria for ALS diagnosis (Brooks et al., 2000). BvFTD-MNDs group of patients did not differ in terms of disease duration from pure bvFTD patients (Mann-Whitney U=39, p=0.803). Similarly, 5 out of 19 ALS patients showed cognitive and/or behavioral disorders (i.e., ALS-FTSD), which however did not satisfy criteria for bvFTD diagnosis (Rascovsky et al., 2011). In detail, three out of these five ALS patients presented with dysexecutive deficits (i.e., ALSci), the other two with apathy, irritability and disinhibition (i.e., ALSbi). Pure ALS and ALS-FTSD did not differ in disease duration (Mann-Whitney U=27, p=0.458) (Table 2).

Table 2. Neuropsychological performances of patients. Scores are corrected according to Italian normative data. Mean and standard deviation (in brackets) for every variable are reported in each group.

	pure ALS (14 patients)	ALS-FTDS (5 patients)	pure bvFTD (14 patients)	bvFTD-MND (6 patients)
Mini Mental Status Examination	27.7 ± 1.2	28.4 ± 1.5	24.5 ± 4.1	23.9 ± 3.4
Verbal Fluency on phonemic cue	26.4 ± 6	28.4 ± 12.5	17.7 ± 9.8	15.8 ± 6
Verbal Fluency on semantic cue	44.2 ± 8.8	43 ± 15.6	29.1 ± 10.7	23.5 ± 10.7
Rey Auditory Verbal Learning test – immediate recall	42.2 ± 7.5	39.5 ± 13.6	31.8 ± 9.6	24.6 ± 14.8
Rey Auditory Verbal Learning test – delayed recall	8.6 ± 2.8	8.5 ± 2.4	5.9 ± 3.8	5.7 ± 4
Rey-Osterrieth Complex Figure – recall	-	-	16.5 ± 8.5	10.2 ± 1.7
Raven Progressive Colored Matrices	32.9 ± 3	29.2 ± 1.7	24.3 ± 6.9	20.9 ± 5.4
Digit Span Forward	5.8 ± 0.4	4.9 ± 1	4.5 ± 1	4.3 ± 1
Wisconsin Card Sorting Test	54.7 ± 28.7	67.7 ± 18	106.1 ± 16.7	104.9 ± 2.1
Cognitive Estimation Task	11.6 ± 2.7	14.4 ± 4.3	14.9 ± 5.3	15.7 ± 8
Stroop test	26.7 ± 8.6	55.1 ± 25.9	48.8 ± 6.9	45 ± 9.3
Rey-Osterrieth Complex Figure – copy	-	-	26.4 ± 4.8	32 ± 4.6
Naming	46.7 ± 1.6	44 ± 1.6	44.2 ± 3	44.7 ± 4.6
Ekman 60-faces task	48 ± 9.4	41.7 ± 7.5	31 ± 8.3	29.75 ± 5.3
Story-based empathy test	15.2 ± 2.3	14.25 ± 3.6	11.3 ± 5.3	10 ± 1.6

3.2 Neurostructural profiles of bvFTD and ALS groups

3.2.1 BvFTD patients versus healthy controls

As expected, VBM whole-brain analyses on GM density revealed a specific pattern of atrophy in bvFTD (whole group, n=20) compared with HC, involving bilateral fronto-temporal and limbic structures. In detail, the pattern of GM density reduction in bvFTD involved the anterior cingulate cortex (ACC), the orbitofrontal cortex and the superior medial frontal gyrus. A significant GM loss was also present in the anterior temporal lobe, including the temporal pole and subcortical regions, such as the amygdala and the hippocampus (Figure 1, panel A).

We found a widespread FA reduction, mainly involving the limbic-prefrontal circuitry, and including the uncinate (UF), inferior fronto-occipital (IFOF), inferior longitudinal (ILF) fasciculi, and the anterior portion of the cingulum bundle (Figure 1, panel B). This pattern also encompassed a consistent FA alteration along the forceps minor, the corpus callosum (CC), the superior longitudinal fasciculus (SLF), the corticospinal tract (CST) and the fornix (cluster size: 30558 voxels, cluster maximum: x=6, y=23, z=14). A corresponding pattern of alteration emerged for MD, which was significantly increased in bvFTD compared to HC (cluster size: 39832 voxels, cluster maximum: x=19, y=40, z=7). Finally, bvFTD showed a relevant change in the mode of anisotropy (MO) in the anterior commissural fibers and in the right CST, the left SLF, the ILF bilaterally and the IFOF.

3.2.2 *ALS patients versus healthy controls*

Compared to HC, ALS (whole group, n=19) showed GM reduction in limbic and orbitofrontal regions, i.e., the ACC bilaterally and the right medial orbital gyrus (Figure 2, panel A).

Whole-brain comparison on microstructural properties between ALS and HC revealed a pattern of FA reduction involving the CC body and the CST bilaterally (cluster size: 1151 voxels, cluster maximum: x=21, y=-21, z=46) (Figure 2, panel B). Additionally, a significant MO decrease along the right CST (cluster size: 45 voxels, cluster maximum: x=21, y=-26, z=41) emerged. ALS did not present significant changes in MD compared to HC.

3.3 Neurostructural conjunction patterns in bvFTD and ALS groups

Voxelwise conjunction analysis between patterns of GM atrophy in bvFTD and ALS (i.e., the overlap between bvFTD<HC and ALS<HC statistical maps) showed a common pattern of GM density reduction involving the ACC bilaterally and the right orbitofrontal cortex (Figure 3, panel A). A one-way ANOVA on mean GM density values extracted from the conjunction cluster highlighted a group effect ($F(2,56)=18.541$, $p<0.00001$). In particular, post-hoc comparisons (Bonferroni correction) revealed significant differences in GM density

among all groups, with lower GM density values in bvFTD compared to both ALS ($p=0.0028$) and HC ($p<0.000001$), and slightly lower GM density values in ALS compared to HC ($p=0.046$).

Voxelwise conjunction analysis between clusters of WM microstructural changes in bvFTD and ALS highlighted a common pattern of alterations, involving FA and MO indices along the CC body and the right CST (Figure 3, panel B) including fibers connecting homologous cortices of supplementary motor, premotor and primary motor areas. A one-way ANOVA (performed separately on mean FA and MO indices extracted from conjunction cluster among the three groups) resulted in a significant group effect (FA: $F(2,56)=15.16$, $p<0.00001$; MO: $F(2,56)=17.19$, $p<0.00001$), showing a consistent pattern. Overall, we found a significant decrease in FA and MO indices within the conjunction cluster in both ALS and bvFTD compared to HC (ALS vs. HC: $p_{FA}<0.00001$; $p_{MO}<0.000001$; bvFTD vs. HC: $p_{FA}=0.0023$; $p_{MO}=0.008$). Notably, post-hoc comparisons (Bonferroni correction) revealed a significant difference between bvFTD and ALS with respect to mean MO values ($p=0.025$), with ALS showing a greater decrease compared to bvFTD, but not in FA ($p=0.189$).

3.4 Neurostructural changes in bvFTD and ALS subgroups

The association analyses aiming to evaluate the strength of the relationship between a) concomitant presence of MNDs and microstructural changes (FA/MO) within the conjunction cluster involving the CST and the CC in bvFTD, and b) concomitant presence of cognitive and/or behavioral symptoms and atrophy within the conjunction cluster (i.e., right medial orbital gyrus and bilateral AAC) in ALS provided no significant results (bvFTD: chi-square=0.159.p=0.69; ALS: chi-square=0.223, p=0.637). In particular, although we detected the presence of reduction of GM density in the bilateral ACC and right medial orbital gyrus in 69% of ALS patients, only 16% of them also displayed cognitive and/or behavioral symptoms. Similarly, while we observed microstructural alterations along the CST and CC in the majority of bvFTD cases (60%), MNDs were found only in 4 out of 12 such patients.

Finally, we performed an exploratory analysis to evaluate possible differences in both GM and WM indices – i.e., GM density and FA/MO respectively – between bvFTD (i.e., pure bvFTD and bvFTD-MNDs) and ALS (i.e., pure ALS and ALS-FTSD) subgroups. Given the small sample size, we calculated the percent variation of neurostructural measures within the significant conjunction cluster among the four patient subgroups and the HC group.

The percent variations analysis on GM density changes showed that bvFTD-MNDs had the most severe GM damage within the conjunction cluster including limbic and orbitofrontal areas (i.e., bilateral ACC and right medial orbital gyrus), while pure bvFTD had intermediate GM density values (greater than the two ALS subgroups), and ALS-FTSD and pure ALS had similar mean values (percent variation <3%). All patient subgroups showed lower GM density values in relation to HC (Table 3).

Table 3. VBM: Percent variations of Grey Matter (GM) density values across the four patient subgroups within limbic and orbitofrontal areas. Percent variations of GM density across patient subgroups have been computed by extracting mean values from the GM conjunction cluster, including the ACC bilaterally and the right medial orbital gyrus. Negative percentages correspond to lower density values (i.e., higher GM reduction) in subgroups listed on rows compared to subgroups listed on columns.

	Pure bvFTD	*Pure ALS*	*ALS-FTSD*	*HC*
bvFTD-MNDs	-4.86%	-14.62%	-17.09%	-22.13%
Pure bvFTD	-	-10.26%	-12.87%	-18.15%
Pure ALS		-	-2.91%	-8.79%
ALS-FTSD			-	-6.06%

ALS = amyotrophic lateral sclerosis; ALS-FTSD = ALS with cognitive and/or behavioral disorders; bvFTD = behavioral variant of frontotemporal dementia; MNDs = motor neuron dysfunctions; HC = healthy controls

Overall, the percent variations analysis on microstructural indices confirmed the ANOVA results. Indeed, FA mean values showed that pure ALS had the most severe diffusion coherence impairment, but percent variations across patient groups were small, ranging from 0.67 to 7.90%. The MO mean indices showed more variability than FA across patient groups, and highlighted that pure ALS had the most severe microstructural impairment along the WM conjunction cluster (right CST and CC body), while ALS-FTSD and bvFTD-MNDs has intermediate FA/MO values, and pure bvFTD had the lowest microstructural damage compared to the other subgroups. All patient subgroups showed lower FA/MO values in relation to HC (Table 4).

Table 4. Percent variations of mean microstructural (FA/MO) values across the four patient subgroups within the corticospinal tract (CST) and corpus callosum (CC). Percent variations of WM microstructure across patient subgroups have been computed by extracting mean values from the WM conjunction cluster, including the CC body and the right CST. Negative percentages correspond to lower FA/MO values (e.g., higher microstructural reduction), and positive percentages correspond to higher FA/MO values (e.g., lower microstructural reduction) in subgroups listed on rows compared to subgroups listed on columns.

		ALS-FTSD	*bvFTD-MNDs*	*Pure bvFTD*	*HC*
Pure ALS	FA	-5.57%	-7.90%	-4.93%	-12.91%
	MO	-46.61%	-37.95%	-67.20%	-76.17%
ALS-FTSD	FA	-	-2.46%	-0.67%	-7.77%
	MO	-	+16.19%	-38.56%	-55.38%
bvFTD-MNDs	FA		-	+3.22%	-5.44%
	MO		-	-47.13%	-61.60%

Pure bvFTD	FA MO			- -	-8.39% -27.37%

ALS = amyotrophic lateral sclerosis; ALS-FTSD = ALS with cognitive and/or behavioral disorders; bvFTD = behavioral variant of frontotemporal dementia; MNDs = motor neuron dysfunctions; HC = healthy controls

4. DISCUSSION

In the present study, we explored the pattern of shared neurostructural alterations within the bvFTD-ALS disease spectrum and their relationship with clinical phenotype. Our results highlighted an overlap of brain changes in bvFTD and ALS in regions encompassing both motor and cognitive networks. The overall findings concerning brain atrophy and microstructural changes are in line with those reported previously (Lillo et al., 2012). However, the overlap patterns reported here suggest that common alterations between ALS and bvFTD can be less widespread in case of pure motor neuron or cognitive diseases. Indeed, we did not find extra-motor damages (e.g., inferior longitudinal fasciculus) in the conjunction pattern between microstructural white-matter features, and nor did we identify commonalities in grey-matter atrophy in the motor cortex. However, in Lillo et al. (2012) the subjects in pure ALS group showed a longer disease course (i.e., disease duration median = 3 years, interquartile range = 1.1-5 years) compared to that of ALS patients in the present study (i.e., median = 18 months, interquartile range = 7.5-29.75 months). This may have crucially affected both GM and WM conjunction patterns. Moreover, the presence of an additional patient group including subjects with combined FTD and ALS diseases may be the reason why they observed larger conjunction patterns.

Specifically, we provided evidence that while the GM conjunction cluster encompasses high-level cognitive fronto-limbic areas (i.e., bilateral ACC and right medial orbital gyrus), the conjunction cluster of WM microstructural alterations involves bundles within the motor system (i.e., the upper portion of the CST and the body of the CC). In a broader perspective, the presence of GM atrophy within the orbital and mesial portions of the prefrontal cortex in

ALS, as well as the WM microstructural changes of motor-related fibers in bvFTD, support the notion of converging pathological processes in ALS and bvFTD (Ahmed et al., 2016). In addition, our study results complement recent findings reporting shared patterns of functional connectivity in ALS and bvFTD (Trojsi et al., 2015). Indeed, the authors described a decreased functional connectivity common to ALS and bvFTD in GM areas involving both sensorimotor (i.e., primary and supplementary motor areas) and cognitive networks, included the salience (i.e., ACC, orbitofrontal and insular regions), as well the executive and the right fronto-parietal networks.

Beside showing the spatial convergence of brain neurostructural degeneration in bvFTD and ALS patients, we evaluated the extent of changes of GM and WM indices within the conjunction clusters in order to explore the severity of neurostructural impairments in patient subgroups according to the presence/absence of specific motor and cognitive/behavioral symptoms. The degree of GM atrophy within the conjunction pattern including fronto-limbic regions resulted significantly more pronounced in bvFTD than ALS patients, and encompassed brain areas typically affected by phosphorylated TPD-43 inclusions in the first stages of the progression of Frontotemporal Lobar Degeneration (Brettschneider et al., 2014). The ACC and right orbitofrontal cortex, consistently detected in neuroimaging studies, are considered the neurostructural markers of bvFTD (Piguet and Hodges, 2013). The presence of ACC atrophy in ALS, indeed, has been related to both apathy (Woolley et al., 2011), and social cognition impairments (Cerami et al., 2013), which are considered some of the key clinical features of bvFTD (Rascovsky et al., 2011). Moreover, since the presence of GM and WM damages in extra-motor brain areas has been detected also in pure ALS (Agosta et al. 2016; Christidi et al., 2017), an early damage of these regions in ALS might represent an early signature of clinical manifestations, including cognitive and/or behavioural impairment, which can arise in the later stages of the disease.

The WM microstructural alterations involve a significant decrease in FA and MO of the CST and CC in both patient groups. These metrics are considered to reflect the orientation of diffusion coherence and the organization of fibers of WM bundles, respectively (e.g., Douaud

et al., 2013, 2011). Within the conjunction clusters we observed different degrees of alteration for FA (whose reduction was comparable among ALS and bvFTD) and MO (showing a greater damage in ALS than in bvFTD). Changes in the microstructural properties of CST and CC are considered early diagnostic biomarkers of ALS (Schuster et al., 2016). Despite the intrinsic heterogeneity of the ALS population, the degeneration of these WM tracts has been consistently observed in several DTI investigations (e.g., Douaud et al., 2011a; Filippini et al., 2010; Turner et al., 2012), and reported in some neuropathological studies (e.g., Smith, 1960). The reduction of the FA index within the CST is a typical and early DTI signature of degenerative processes involving the upper motor neurons in ALS patients (Turner et al., 2009), while the damage of the CC is probably related to either the interhemispheric spread of the neurodegenerative process or to a secondary and independent degenerative event (Filippini et al., 2010). Accordingly, the presence of changes in CC and CST in bvFTD strongly suggests a motor neuron dysfunction also in this group of patients. This evidence is further supported by previous neuroimaging studies (Daianu et al., 2015; Lillo et al., 2012; Mahoney et al., 2014; Whitwell et al., 2010; Zhang et al., 2009).

Overall, our results provide further support to the hypothesis of ALS-FTD pathological continuum. In particular, about a decade ago it has been proposed that a large part of bvFTD – as well as other clinical manifestations within the Frontotemporal Lobar Degeneration (FTLD) spectrum – and the majority of sporadic cases of ALS should be considered two divergent expressions of a unique pathological spectrum centered on the 43kDa TAR DNA-binding protein (TDP-43) proteinopathy (Neumann et al., 2006). This view has been recently corroborated by neuropathological investigations describing a time-sequential propagation of neurostructural alterations induced by the spread of phosphorylated TDP-43 aggregates in sporadic ALS (Brettschneider et al., 2013), which partially converges with the pathological spread pattern observed in bvFTD (Brettschneider et al., 2014). In bvFTD the degenerative process starts in the orbital and anterior portions of the prefrontal cortex, spreads caudally to the lateral and anteromedial parts of the frontal lobe, then to the limbic structures, brainstem nuclei, sensorimotor cortices, parietal lobes, lower motor

neurons, and finally reaches the occipital lobe (Brettschneider et al., 2014). In ALS, the dissemination of TDP-43 aggregates starts from the motor cortices, the somatomotor nuclei of the brainstem, and the lower motor neurons. Then, the pathological changes disseminate to the reticular formation and precerebellar nuclei, and later to the prefrontal (i.e., gyrus rectus and orbital gyri) and postcentral cortices the striatum, and the medial temporal lobe structures (Brettschneider et al., 2013). In line with our results, recent MRI studies on large samples of ALS (Müller et al., 2016; Schulthess et al., 2016) confirmed *in vivo* the spreading pattern of neuropathological changes reported by Brettschneider et al. (2013). Indeed, Muller et al. (2016) proposed a model of DTI-based tract-wise progression pattern in ALS, according to a neuropathological staging scheme and associated to disease severity, starting from motor network and disseminating to extra-motor brain regions (i.e., frontal and hippocampal regions, brainstem). Comparably, Schulthess and colleagues (Schulthess et al., 2016) reported a sequential involvement of functional networks remarkably resembling the distribution of TDP-43 pathology.

In the present *in vivo* study, the neurostructural findings strongly support a convergence of the TDP-43-like proteinopathy dissemination between specific commonly involved brain regions in ALS and bvFTD. In particular, the quantification of GM and WM damages within common altered structures in patient groups unveiled two different trends, based on the classification of patients in terms of the presence/absence of MNDs and of cognitive and/or behavioral symptoms. The first trend concerns a higher degree of atrophy in orbitofrontal and frontomedial regions in patients with more severe cognitive and/or behavioral symptoms. In particular, the reduction of GM density in the right orbitofrontal cortex and bilateral ACC resulted more severe in bvFTD-MNDs than in other patient groups, with ALS-FTSD and pure ALS showing similar values. Conversely, the second trend highlights a higher degree of degeneration in the motor pathway in patients with more severe motor neuron disorders. Specifically, the diffusion orientation coherence (FA) within CC and CST is on average lower in pure ALS, with ALS-FTSD, bvFTD-MNDs and pure bvFTD having smaller but similar damages. Additionally, microstructural changes affecting the shape

of the diffusion tensor (MO), and reflecting an altered organization of WM fibers, revealed a continuum of alterations ranging from pure ALS (i.e., more severe alteration in relation to other patient groups) to pure bvFTD (i.e., less severe alteration than other patient groups), with ALS-FTSD and bvFTD-MNDs having intermediate values.

In the present sample, however, the involvement of the right orbitofrontal cortex and bilateral ACC in ALS was independent of the presence of cognitive and/or behavioral symptoms, as half of ALS sample showed a morphometrical alteration of these brain regions in absence of extra-motor clinical manifestations. Similarly, we found that the presence of MNDs was independent from the microstructural alterations along the CST/CC. In this regard, previous investigations identified extra-motor alterations in ALS without cognitive impairment (e.g., Agosta et al., 2016; Christidi et al., 2017), as well as the presence of motor alteration in bvFTD without clinical manifestation of MND (e.g., Lillo et al. 2012; Trojsi et al., 2015). Taken together, these findings might indicate the presence of structural changes antedating clinical manifestations.

Conversely, the presence of cognitive and/or behavioral impairments or MNDs without the alteration of the corresponding neurostructural substrate found in some cases (i.e., absence of either extra-motor degeneration in ALS-FTSD or CST/CC damage in bvFTD-MNDs) might be due to the presence of subtle dysfunctions reflected in a defective functional connectivity within networks regulating cognitive or sensorimotor processes. However, further structural and functional neuroimaging studies are needed to clarify this issue.

A major limitation of the present study is related to the sample size of patient subgroups, which did not allow us to perform formal statistical comparisons, but only a description in terms of percent variations of GM and WM damages (bvFTD, bvFTD-MNDs, ALS and ALS-FTSD). Of course this can affect the estimate of the actual magnitude of the difference observed among subgroups, but the consistency between our data and previous neuropathological (Brettschneider et al., 2013, 2014) and neuroimaging (Müller et al., 2016; Schulthess et al., 2016) reports strengthens the present results. Nevertheless, although the small size of our patient subgroups prevents us from drawing robust inferences, the

quantification of neurostructural alterations across ALS and bvFTD subgroups can provide novel clues into the converging anatomical changes within the disease spectrum, and paves the way for further in-depth investigations.

5. CONCLUSIONS

Altogether, the present data provide new *in vivo* evidence of converging sequential pathological dissemination patterns in ALS and bvFTD. These neurodegenerative proteinopathies share in the majority of cases common pathways of pathology propagation, entailing both macro- and microstructural alterations, but following different courses.

First, the common pattern of macrostructural damage involving fronto-limbic structures (i.e., right medial orbital gyrus and bilateral ACC) corroborates the presence of subtle *bvFTD-like* disorders in ALS patients. Then, the shared microstructural damage affecting the corticospinal and commissural (i.e., corpus callosum) fibers indicates a subclinical *ALS-like* motor neuron degeneration in bvFTD. In addition, the quantification of such neurostructural changes reveals the presence of a higher degree of degeneration in the motor pathway in bvFTD patients with clinical or electromyographical evidence of motor neuron dysfunction, as well as a higher degree of atrophy of orbitofrontal and fronto-medial regions in ALS patients with neuropsychological evidence of frontotemporal dysfunction.

In conclusion, although further clinical, neuroimaging and neuropathological studies based on larger samples are needed to reach more conclusive findings, the present *in vivo* imaging study provide a step forward a better comprehension of the bidirectional spreading pattern of neurodegenerative changes occurring within the ALS-FTD spectrum.

Acknowledgments: We thank Dr. V. Golzi, Dr. A. Marcone, Dr. M.C. Giusti and Dr. M. Zamboni for patient recruitment.

Funding: This work was supported by a Ministry for Instruction, University and Research (MIUR) grant (PRIN 2010XPMFW4_008; I meccanismi neurocognitivi alla base delle interazioni sociali).

References

Abrahams, S., Goldstein, L.H., Suckling, J., Ng, V., Simmons, A., Chitnis, X., Atkins, L., Williams, S.C.R., Leigh, P.N., 2005. Frontotemporal white matter changes in amyotrophic lateral sclerosis. J. Neurol. 252, 321–331. doi:10.1007/s00415-005-0646-x

Agosta, F., Ferraro, P.M., Riva, N., Spinelli, E.G., Chiò, A., Canu, E., Valsasina, P., Lunetta, C., Iannaccone, S., Copetti, M., Prudente, E., Comi, G., Falini, A., Filippi, M., 2016. Structural brain correlates of cognitive and behavioral impairment in MND. Hum. Brain Mapp. 37, 1614–1626. doi:10.1002/hbm.23124

Ahmed, R.M., Irish, M., Piguet, O., Halliday, G.M., Ittner, L.M., Farooqi, S., Hodges, J.R., Kiernan, M.C., 2016. Amyotrophic lateral sclerosis and frontotemporal dementia: distinct and overlapping changes in eating behaviour and metabolism. Lancet. Neurol. doi:10.1016/S1474-4422(15)00380-4

Ashburner, J., 2009. Computational anatomy with the SPM software. Magn. Reson. Imaging. doi:10.1016/j.mri.2009.01.006

Ashburner, J., 2007. A fast diffeomorphic image registration algorithm. Neuroimage 38, 95–113. doi:10.1016/j.neuroimage.2007.07.007

Brettschneider, J., Del Tredici, K., Irwin, D.J., Grossman, M., Robinson, J.L., Toledo, J.B., Fang, L., Van Deerlin, V.M., Ludolph, A.C., Lee, V.M.Y., Braak, H., Trojanowski, J.Q., 2014. Sequential distribution of pTDP-43 pathology in behavioral variant frontotemporal dementia (bvFTD). Acta Neuropathol. 127, 423–439. doi:10.1007/s00401-013-1238-y

Brettschneider, J., Del Tredici, K., Toledo, J.B., Robinson, J.L., Irwin, D.J., Grossman, M., Suh, E., Van Deerlin, V.M., Wood, E.M., Baek, Y., Kwong, L., Lee, E.B., Elman, L., McCluskey, L., Fang, L., Feldengut, S., Ludolph, A.C., Lee, V.M.Y., Braak, H.,

Trojanowski, J.Q., 2013. Stages of pTDP-43 pathology in amyotrophic lateral sclerosis. Ann. Neurol. 74, 20–38. doi:10.1002/ana.23937

Brooks, B.R., Miller, R.G., Swash, M., Munsat, T.L., 2000. El Escorial revisited: revised criteria for the diagnosis of amyotrophic lateral sclerosis. Amyotroph. Lateral Scler. Other Motor Neuron Disord. 1, 293–299. doi:DOI 10.1080/146608200300079536

Burrell, J.R., Kiernan, M.C., Vucic, S., Hodges, J.R., 2011. Motor Neuron dysfunction in frontotemporal dementia. Brain 134, 2582–2594. doi:10.1093/brain/awr195

Cedarbaum, J.M., Stambler, N., Malta, E., Fuller, C., Hilt, D., Thurmond, B., Nakanishi, A., 1999. The ALSFRS-R: A revised ALS functional rating scale that incorporates assessments of respiratory function. J. Neurol. Sci. 169, 13–21. doi:10.1016/S0022-510X(99)00210-5

Cerami, C., Dodich, A., Canessa, N., Crespi, C., Iannaccone, S., Corbo, M., Lunetta, C., Consonni, M., Scola, E., Falini, A., Cappa, S.F., 2013. Emotional empathy in amyotrophic lateral sclerosis: a behavioural and voxel-based morphometry study. doi:10.3109/21678421.2013.785568

Cerami, C., Marcone, A., Crespi, C., Iannaccone, S., Marangoni, C., Dodich, A., Giusti, M.C., Zamboni, M., Golzi, V., Cappa, S.F., 2015a. Motor neuron dysfunctions in the frontotemporal lobar degeneration spectrum: A clinical and neurophysiological study. J. Neurol. Sci. doi:10.1016/j.jns.2015.02.039

Cerami, C., Marcone, A., Crespi, C., Iannaccone, S., Marangoni, C., Dodich, A., Giusti, M.C., Zamboni, M., Golzi, V., Cappa, S.F., 2015b. Motor neuron dysfunctions in the frontotemporal lobar degeneration spectrum: a clinical and neurophysiological study. doi:10.1016/j.jns.2015.02.039

Consonni, M., Iannaccone, S., Cerami, C., Frasson, P., Lacerenza, M., Lunetta, C., Corbo, M., Cappa, S.F., 2013. The cognitive and behavioural profile of Amyotrophic Lateral Sclerosis: Application of the consensus criteria. Behav. Neurol. 27, 143–153. doi:10.3233/BEN-2012-110202

Daianu, M., Mendez, M.F., Baboyan, V.G., Jin, Y., Melrose, R.J., Jimenez, E.E., Thompson,

P.M., 2015. An advanced white matter tract analysis in frontotemporal dementia and early-onset Alzheimer???s disease. Brain Imaging Behav. doi:10.1007/s11682-015-9458-5

Devenney, E., Vucic, S., Hodges, J.R., Kiernan, M.C., 2015. Motor neuron disease-frontotemporal dementia: a clinical continuum. Expert Rev. Neurother. 15, 509–522. doi:10.1586/14737175.2015.1034108

Douaud, G., Filippini, N., Knight, S., Talbot, K., Turner, M.R., 2011a. Integration of structural and functional magnetic resonance imaging in amyotrophic lateral sclerosis. Brain 134, 3470–9. doi:10.1093/brain/awr279

Douaud, G., Jbabdi, S., Behrens, T.E.J., Menke, R.A., Gass, A., Monsch, A.U., Rao, A., Whitcher, B., Kindlmann, G., Matthews, P.M., Smith, S., 2011b. DTI measures in crossing-fibre areas: Increased diffusion anisotropy reveals early white matter alteration in MCI and mild Alzheimer's disease. Neuroimage 55, 880–890. doi:10.1016/j.neuroimage.2010.12.008

Douaud, G., Menke, R. a L., Gass, A., Monsch, A.U., Rao, A., Whitcher, B., Zamboni, G., Matthews, P.M., Sollberger, M., Smith, S., 2013. Brain microstructure reveals early abnormalities more than two years prior to clinical progression from mild cognitive impairment to Alzheimer's disease. J. Neurosci. 33, 2147–55. doi:10.1523/JNEUROSCI.4437-12.2013

Eickhoff, S.B., Stephan, K.E., Mohlberg, H., Grefkes, C., Fink, G.R., Amunts, K., Zilles, K., 2005. A new SPM toolbox for combining probabilistic cytoarchitectonic maps and functional imaging data. Neuroimage 25, 1325–1335. doi:10.1016/j.neuroimage.2004.12.034

Ferrari, R., Kapogiannis, D., Huey, E.D., Momeni, P., 2011. FTD and ALS: a tale of two diseases. Curr. Alzheimer Res. 8, 273–94. doi:10.2174/156720511795563700

Filippini, N., Douaud, G., MacKay, C.E., Knight, S., Talbot, K., Turner, M.R., 2010. Corpus callosum involvement is a consistent feature of amyotrophic lateral sclerosis. Neurology 75, 1645–1652. doi:10.1212/WNL.0b013e3181fb84d1

Goldstein, L.H., Abrahams, S., 2013. Changes in cognition and behaviour in amyotrophic lateral sclerosis: Nature of impairment and implications for assessment. Lancet Neurol. doi:10.1016/S1474-4422(13)70026-7

Hua, K., Zhang, J., Wakana, S., Jiang, H., Li, X., Reich, D.S., Calabresi, P.A., Pekar, J.J., van Zijl, P.C.M., Mori, S., 2008. Tract probability maps in stereotaxic spaces: Analyses of white matter anatomy and tract-specific quantification. Neuroimage 39, 336–347. doi:10.1016/j.neuroimage.2007.07.053

Lattante, S., Ciura, S., Rouleau, G.A., Kabashi, E., 2015. Defining the genetic connection linking amyotrophic lateral sclerosis (ALS) with frontotemporal dementia (FTD). Trends Genet. doi:10.1016/j.tig.2015.03.005

Lillo, P., Mioshi, E., Burrell, J.R., Kiernan, M.C., Hodges, J.R., Hornberger, M., 2012. Grey and White Matter Changes across the Amyotrophic Lateral Sclerosis-Frontotemporal Dementia Continuum. PLoS One 7. doi:10.1371/journal.pone.0043993

Ling, S.C., Polymenidou, M., Cleveland, D.W., 2013. Converging mechanisms in als and FTD: Disrupted RNA and protein homeostasis. Neuron. doi:10.1016/j.neuron.2013.07.033

Lomen-Hoerth, C., 2011. Clinical phenomenology and neuroimaging correlates in ALS-FTD, in: Journal of Molecular Neuroscience. pp. 656–662. doi:10.1007/s12031-011-9636-x

Lomen-Hoerth, C., Anderson, T., Miller, B., 2002. The overlap of amyotrophic lateral sclerosis and frontotemporal dementia. Neurology 59, 1077–1079. doi:10.1097/WCO.0b013e3283168d1d

Mahoney, C.J., Ridgway, G.R., Malone, I.B., Downey, L.E., Beck, J., Kinnunen, K.M., Schmitz, N., Golden, H.L., Rohrer, J.D., Schott, J.M., Rossor, M.N., Ourselin, S., Mead, S., Fox, N.C., Warren, J.D., 2014. Profiles of white matter tract pathology in frontotemporal dementia. Hum. Brain Mapp. 35, 4163–4179. doi:10.1002/hbm.22468

Müller, H.-P., Turner, M.R., Grosskreutz, J., Abrahams, S., Bede, P., Govind, V., Prudlo, J., Ludolph, A.C., Filippi, M., Kassubek, J., 2016. A large-scale multicentre cerebral diffusion tensor imaging study in amyotrophic lateral sclerosis. J. Neurol. Neurosurg.

Psychiatry jnnp-2015-311952. doi:10.1136/jnnp-2015-311952

Neumann, M., Sampathu, D.M., Kwong, L.K., Truax, A.C., Micsenyi, M.C., Chou, T.T., Bruce, J., Schuck, T., Grossman, M., Clark, C.M., McCluskey, L.F., Miller, B.L., Masliah, E., Mackenzie, I.R., Feldman, H., Feiden, W., Kretzschmar, H. a, Trojanowski, J.Q., Lee, V.M.-Y., 2006. Ubiquitinated TDP-43 in frontotemporal lobar degeneration and amyotrophic lateral sclerosis. Science 314, 130–3. doi:10.1126/science.1134108

Nichols, T., Brett, M., Andersson, J., Wager, T., Poline, J.B., 2005. Valid conjunction inference with the minimum statistic. Neuroimage 25, 653–660. doi:10.1016/j.neuroimage.2004.12.005

Phukan, J., Elamin, M., Bede, P., Jordan, N., Gallagher, L., Byrne, S., Lynch, C., Pender, N., Hardiman, O., 2012. The syndrome of cognitive impairment in amyotrophic lateral sclerosis: a population-based study. J. Neurol. Neurosurg. Psychiatry 83, 102–8. doi:10.1136/jnnp-2011-300188

Piguet, O., Hodges, J.R., 2013. Behavioural-variant frontotemporal dementia: an update. Dement. Neuropsychol. 7, 10–18.

Rascovsky, K., Hodges, J.R., Knopman, D., Mendez, M.F., Kramer, J.H., Neuhaus, J., Van Swieten, J.C., Seelaar, H., Dopper, E.G.P., Onyike, C.U., Hillis, A.E., Josephs, K.A., Boeve, B.F., Kertesz, A., Seeley, W.W., Rankin, K.P., Johnson, J.K., Gorno-Tempini, M.L., Rosen, H., Prioleau-Latham, C.E., Lee, A., Kipps, C.M., Lillo, P., Piguet, O., Rohrer, J.D., Rossor, M.N., Warren, J.D., Fox, N.C., Galasko, D., Salmon, D.P., Black, S.E., Mesulam, M., Weintraub, S., Dickerson, B.C., Diehl-Schmid, J., Pasquier, F., Deramecourt, V., Lebert, F., Pijnenburg, Y., Chow, T.W., Manes, F., Grafman, J., Cappa, S.F., Freedman, M., Grossman, M., Miller, B.L., 2011. Sensitivity of revised diagnostic criteria for the behavioural variant of frontotemporal dementia. Brain 134, 2456–2477. doi:10.1093/brain/awr179

Ringholz, G.M., Appel, S.H., Bradshaw, M., Cooke, N.A., Mosnik, D.M., Schulz, P.E., 2005. Prevalence and patterns of cognitive impairment in sporadic ALS. Neurology 65, 586–590. doi:10.1212/01.wnl.0000172911.39167.b6

Schulthess, I., Gorges, M., Müller, H.-P., Lulé, D., Del Tredici, K., Ludolph, A.C., Kassubek, J., 2016. Functional connectivity changes resemble patterns of pTDP-43 pathology in amyotrophic lateral sclerosis. Sci. Rep. 6, 38391. doi:10.1038/srep38391

Schuster, C., Elamin, M., Hardiman, O., Bede, P., 2016. The segmental diffusivity profile of amyotrophic lateral sclerosis associated white matter degeneration. Eur. J. Neurol. 23, 1361–1371. doi:10.1111/ene.13038

Seeley, W.W., Crawford, R., Rascovsky, K., Kramer, J.H., Weiner, M., Miller, B.L., Gorno-Tempini, M.L., 2008. Frontal paralimbic network atrophy in very mild behavioral variant frontotemporal dementia. Arch. Neurol. 65, 249–255. doi:10.1001/archneurol.2007.38

Smith, S.M., Jenkinson, M., Johansen-Berg, H., Rueckert, D., Nichols, T.E., Mackay, C.E., Watkins, K.E., Ciccarelli, O., Cader, M.Z., Matthews, P.M., Behrens, T.E.J., 2006. Tract-based spatial statistics: Voxelwise analysis of multi-subject diffusion data. Neuroimage 31, 1487–1505. doi:10.1016/j.neuroimage.2006.02.024

Smith, S.M., Nichols, T.E., 2009. Threshold-free cluster enhancement: Addressing problems of smoothing, threshold dependence and localisation in cluster inference. Neuroimage 44, 83–98. doi:10.1016/j.neuroimage.2008.03.061

Strong, M.J., Abrahams, S., Goldstein, L.H., Woolley, S., Mclaughlin, P., Snowden, J., Mioshi, E., Roberts-South, A., Benatar, M., HortobáGyi, T., Rosenfeld, J., Silani, V., Ince, P.G., Turner, M.R., 2017. Amyotrophic lateral sclerosis - frontotemporal spectrum disorder (ALS-FTSD): Revised diagnostic criteria. Amyotroph. Lateral Scler. Front. Degener. 0, 1–22. doi:10.1080/21678421.2016.1267768

Strong, M.J., Grace, G.M., Freedman, M., Lomen-Hoerth, C., Woolley, S., Goldstein, L.H., Murphy, J., Shoesmith, C., Rosenfeld, J., Leigh, P.N., Bruijn, L., Ince, P., Figlewicz, D., 2009. Consensus criteria for the diagnosis of frontotemporal cognitive and behavioural syndromes in amyotrophic lateral sclerosis. Amyotroph. Lateral Scler. 10, 131–146. doi:Pii 907462414\rDoi 10.1080/17482960802654364

Trojsi, F., Esposito, F., de Stefano, M., Buonanno, D., Conforti, F.L., Corbo, D., Piccirillo,

G., Cirillo, M., Monsurrò, M.R., Montella, P., Tedeschi, G., 2015. Functional overlap and divergence between ALS and bvFTD. Neurobiol. Aging 36, 413–423. doi:10.1016/j.neurobiolaging.2014.06.025

Tsermentseli, S., Leigh, P.N., Goldstein, L.H., 2012. The anatomy of cognitive impairment in amyotrophic lateral sclerosis: More than frontal lobe dysfunction. Cortex. doi:10.1016/j.cortex.2011.02.004

Turner, M.R., Agosta, F., Govind, V., Bede, P., Lulé, D., Verstraete, E., 2012. Neuroimaging in amyotrophic lateral sclerosis Review. Biomarkers Med. 6, 319–337. doi:10.2217/bmm.12.26

Turner, M.R., Kiernan, M.C., Leigh, P.N., Talbot, K., 2009. Biomarkers in amyotrophic lateral sclerosis. Lancet Neurol. doi:10.1016/S1474-4422(08)70293-X

Turner, M.R., Verstraete, E., 2015. What does imaging reveal about the pathology of amyotrophic lateral sclerosis? Curr. Neurol. Neurosci. Rep. 15, 569. doi:10.1007/s11910-015-0569-6

Weishaupt, J.H., Hyman, T., Dikic, I., 2016. Common Molecular Pathways in Amyotrophic Lateral Sclerosis and Frontotemporal Dementia. Trends Mol. Med. doi:10.1016/j.molmed.2016.07.005

Whitwell, J.L., Avula, R., Senjem, M.L., Kantarci, K., Weigand, S.D., Samikoglu, A., Edmonson, H.A., Vemuri, P., Knopman, D.S., Boeve, B.F., Petersen, R.C., Josephs, K.A., Jack, C.R., 2010. Gray and white matter water diffusion in the syndromic variants of frontotemporal dementia. Neurology 74, 1279–1287. doi:10.1212/WNL.0b013e3181d9edde

Woolley, S.C., Zhang, Y., Schuff, N., Weiner, M.W., Katz, J.S., 2011. Neuroanatomical correlates of apathy in ALS using 4 Tesla diffusion tensor MRI. Amyotroph. Lateral Scler. 12, 52–58. doi:10.3109/17482968.2010.521842

Zhang, Y., Schuff, N., Du, A.-T., Rosen, H.J., Kramer, J.H., Gorno-Tempini, M.L., Miller, B.L., Weiner, M.W., 2009. White matter damage in frontotemporal dementia and Alzheimer's disease measured by diffusion MRI. Brain 132, 2579–92.

doi:10.1093/brain/awp071

Figure Legends

Figure 1. Neurostructural profile of bvFTD vs. HC

A: Whole-brain results from VBM highlight, in bvFTD patients compared to HC, significantly decreased GM density in fronto-temporal and limbic structures bilaterally ($p<0.05$, FWE-corrected). The statistical map is superimposed on the MNI T1 template. B: Whole-brain results from TBSS highlight, in bvFTD patients compared to HC, significantly decreased FA and MO, as well as significantly increased MD, in the limbic-prefrontal circuitry ($p<0.05$, FWE-corrected). The statistical maps are superimposed on FMRIB standard-space FA template.

Figure 2. Neurostructural profile of ALS vs. HC

A: Whole-brain results from VBM highlight, in ALS patients compared to HC, significantly decreased GM density in the bilateral ACC and right medial orbital gyrus. The statistical map is superimposed on the MNI T1 template. B: Whole-brain results from TBSS highlight, in ALS patients compared to HC, significantly decreased FA and MO in the CST and the body of CC bilaterally ($p<0.05$, FWE-corrected). The statistical maps are superimposed on FMRIB standard-space FA template.

Figure 3. Neurostructural conjunction pattern common to bvFTD and ALS

A: Whole-brain conjunction analysis of GM density highlights, in bvFTD and ALS groups, a common pattern of alterations involving the bilateral ACC and the right orbitofrontal cortex ($p<0.05$, FWE-corrected). The statistical map is superimposed on the MNI T1 template. B: Whole-brain conjunction analysis of WM microstructural characteristics highlights, in bvFTD and ALS groups, a common pattern of alterations involving a significant decrease of both FA and MO indices within the right CST and the body of the CC ($p<0.05$, FWE-corrected). The statistical maps are superimposed on FMRIB standard-space FA template.

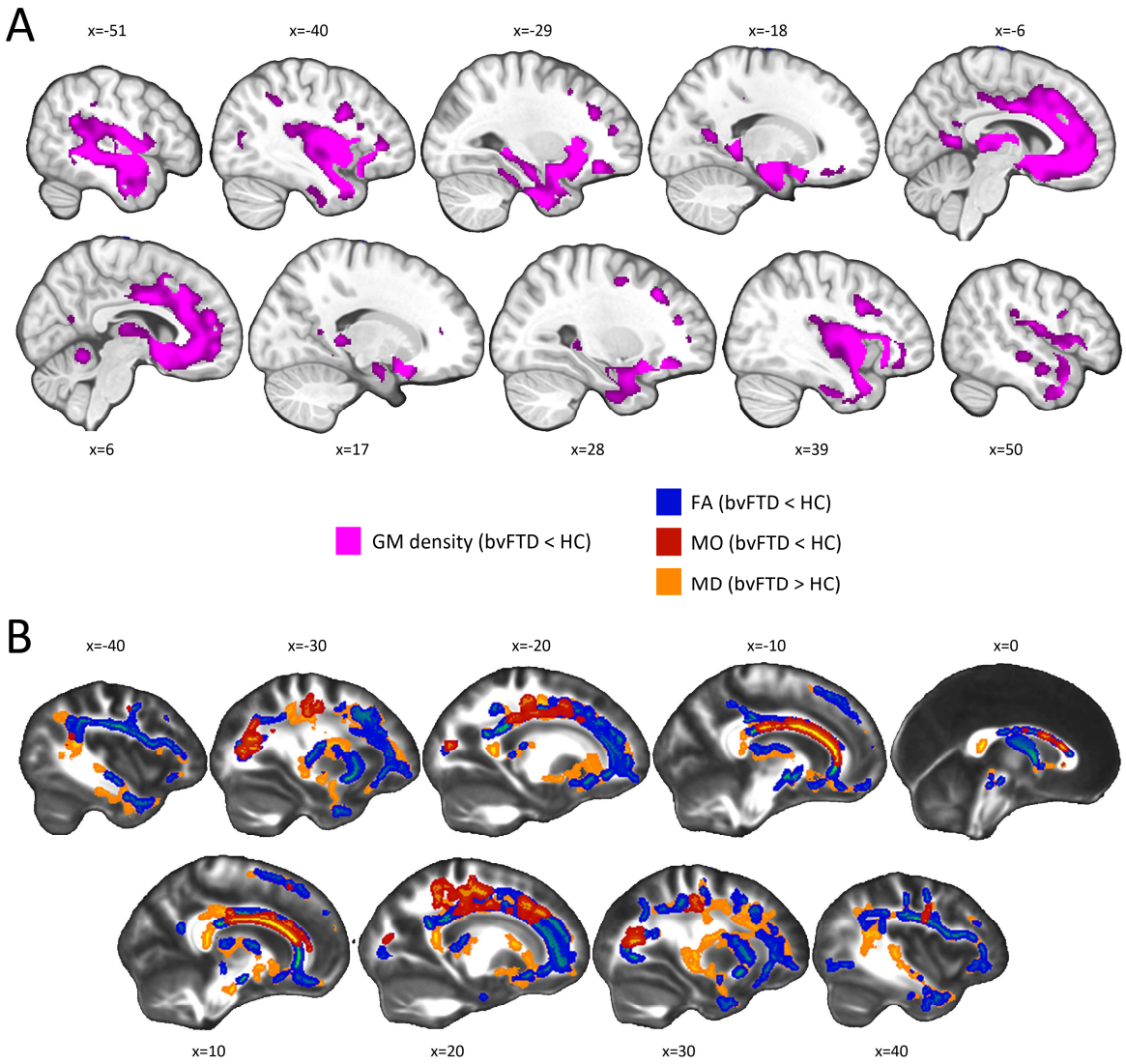

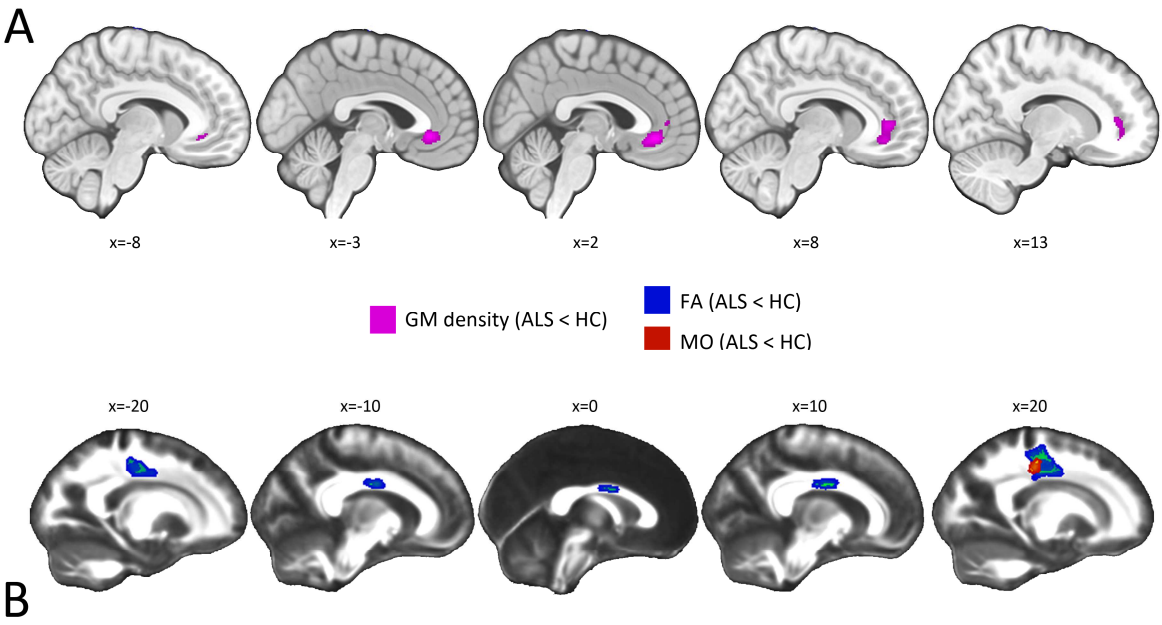

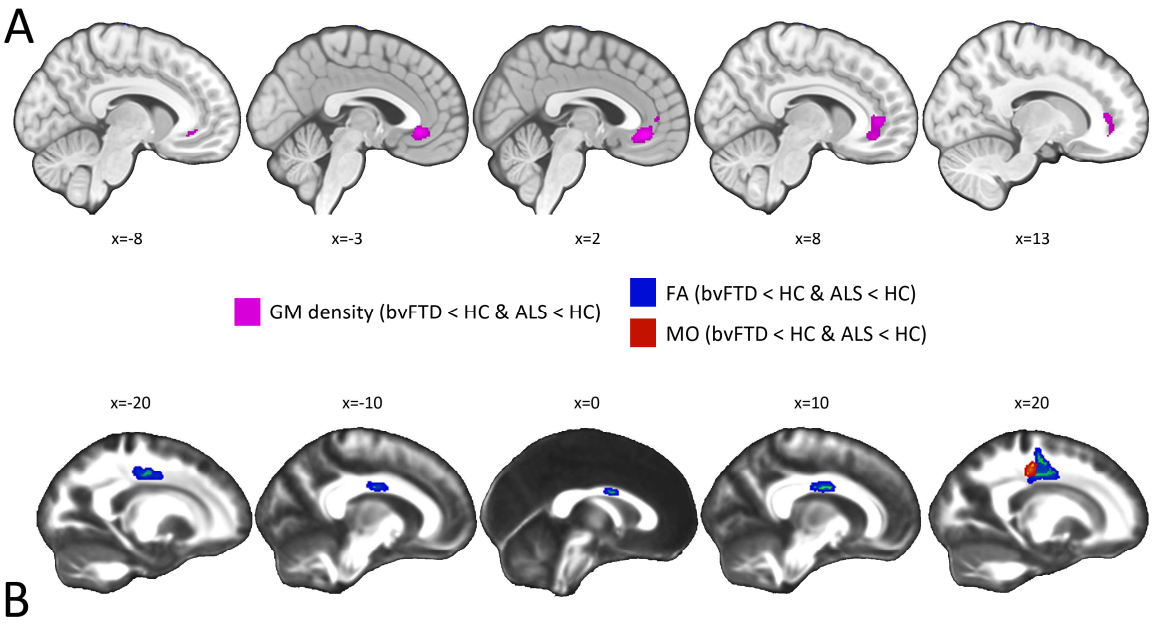

Highlights

ALS and bvFTD share a common pattern of WM and GM alterations

Higher degree of WM degeneration is reflected in more severe motor neuron disorders

GM atrophy is greater in presence of more severe executive and/or behavioral symptoms

Motor pathway damage in bvFTD may indicate a subtle ALS-like motor neuron dysfunction

Fronto-limbic atrophy in ALS may suggest the presence of subtle bvFTD-like symptoms